Effect of Pressure on the Proton Transfer Rate from a Photoacid to a Solvent. 4. Photoacids in Methanol

Liat Genosar, Tatiana Lasitza, Rinat Gepshtein, Pavel Leiderman, Nahum Koifman, and Dan Huppert*

Raymond and Beverly Sackler Faculty of Exact Sciences, School of Chemistry, Tel Aviv University, Tel Aviv 69978, Israel

Received: February 22, 2005; In Final Form: April 4, 2005

The pressure dependence of the excited-state proton dissociation rate constant of four photoacids, 2-naphthol-6,8-disulfonate (2N68DS), 10-hydroxycamptothecin (10-CPT), 5-cyano-2-naphthol (5CN2), and 5,8-dicyano-2-naphthol (DCN2), are studied in methanol. The results are compared with the results of the pressure dependence study we recently conducted for several photoacids in water, ethanol, and propanol. The pressure dependence is explained using an approximate stepwise two-coordinate proton transfer model. The increase in rate, as a function of pressure, manifests a strong dependence of proton tunneling on the distance which decreases with an increase of pressure between the two oxygen atoms involved in the process. The decrease in the proton transfer rate with increasing pressure reflects the dependence of the reaction on the solvent relaxation rate. We found that, for the relatively weak photoacids 2N68DS, 10-CPT, and 5CN2, the proton transfer rate constant increases by a factor of about 5−8 at a pressure of about 1.5 GPa. For a strong photoacid like DCN2, the rate increase was only by a factor of 2.

Introduction

Proton transfer to a solvent (PTTS) is a fundamental process in chemistry and biology.[1,2] Intermolecular excited-state proton transfer (ESPT) from a photoacid molecule, that dissociates upon excitation to produce an excited anion and a proton,[3−10] was extensively studied by steady-state as well as time-resolved techniques in liquids and solids. Recent studies[11−18] emphasize the dual role played by the solvent molecule (1) as a proton acceptor and (2) as a solvating medium of both the reactant and the product.[19−21]

Theoretical studies revealed that tunneling is the dominant reaction mode for proton transfer, even at ambient temperatures.[22−29] These theories show that the presence of a potential energy barrier in the proton reaction coordinate causes tunneling through the barrier in the reaction pathway, as opposed to passage over the barrier.

Pressure is known to influence the rate of chemical reactions in the condensed phase. External pressure changes such properties of the medium as compressibility, viscosity, and the reorganization energy of the medium.[30] It also modifies the reactivity by changing the reaction free volume and the potential energy profile along the reaction path. The absolute value of the reaction rate constant and its pressure dependence can depend on all these parameters. The pressure influences the characteristics of both the classical over-barrier reactions and the under-the-barrier reaction where tunneling is the mechanism of proton transfer to the proton acceptor. The pressure influence on tunneling in the solid state is discussed in refs 30 and 31. In solids, the tunneling reaction depends exponentially on both the equilibrium distance between the reactants and the frequency of intermolecular vibrations, which varies with compression.

In previous papers,[14−18,32−35] we described our experimental results of temperature and pressure dependence of the excited-state proton transfer from a photoacid to protic liquid solvents such as water and alcohols (monols, diols, and glycerol).

We proposed a simple stepwise model to describe and calculate both the temperature and pressure dependence of the proton transfer to the solvent reaction. The model accounts for the large difference in the temperature dependence of the proton transfer rate at high and low temperatures. At low temperatures, the proton transfer rate depends on the solvent relaxation rate. The model also accounts for the dependence of the proton transfer rate on pressure.[32−34] In water, pressure increases the proton transfer rate. At about 10 kbar, the freezing point of water at room temperature, for a large number of photoacids, the rate increases approximately tenfold. For both ethanol and propanol, the proton transfer rate first increases with a pressure increase. At pressures above 0.5 and 0.76 GPa in propanol and ethanol, respectively, the rate decreases with a further increase in pressure. In the stepwise model, which will be described in the discussion section, the proton transfer reaction depends on two coordinates, the first of which depends on the generalized solvent configuration. The solvent coordinate characteristic time is within the range of the dielectric relaxation time, τ_D, and the longitudinal relaxation, τ_L $(\epsilon_s/\epsilon_\infty)\tau_D$, where ϵ_s and ϵ_∞ are the static and high-frequency dielectric constants, respectively. The second coordinate is the actual proton translational motion (tunneling) along the reaction path. The model restricts the proton transfer process to a stepwise one. The proton moves to the adjacent hydrogen-bonded solvent molecule only when the solvent configuration brings the system to the crossing point.

One important difference between electron transfer and proton transfer is the extreme sensitivity of the proton tunneling matrix element to distance. The functional form of the tunneling coupling matrix element, C, between the reactant and product states, for moderate to weak coupling, is[24]

$$C(q_H) = C_0 \exp(-\alpha\delta q_H) \qquad (1)$$

The decay parameter, α, is very large, 25−35 Å^{-1}, in comparison with the corresponding decay parameter for the

* Corresponding author. E-mail: huppert@tulip.tau.ac.il. Fax/phone: 972-3-6407012.

10.1021/jp050926z CCC: $30.25
Published on Web 05/07/2005

electronic coupling in electron transfer, 1 $Å^{-1}$. It is this feature that makes the dynamics of proton transfer so sensitive to the internuclear separation of the two heavy atoms, and hence, pressure can be used to gradually change the intermolecular distance. For many liquids, pressure is known to change the liquid and solid densities. For methanol and ethanol, the volume decreases by about 25% at about 10 kbar. As the volume decreases with pressure, so does the intermolecular distance. The model was successfully applied to explain the temperature and pressure dependence of the excited-state intermolecular proton transfer of several compounds in several protic liquids (ESPT).

In this study, we further explore the effect of pressure on ESPT dynamics in methanol. For this purpose, we chose four photoacids: 2-naphthol-6,8-disulfonate (2N68DS), 10-hydroxy-camptothecin (10-CPT), 5-cyano-2-naphthol (5CN2), and 5,8-dicyano-2-naphthol (DCN2).

In water, the rate of proton transfer increases tenfold with pressure. In ethanol and propanol, the rate first increases with pressure increase, but at pressures larger than 0.5 GPa, the rate decreases as the pressure increases further. The solvent methanol is a protic solvent, closest to water in its protic properties such as excess proton conductivity and fast proton transfer rate in the ESPT process. The solvent relaxation rate of methanol is faster than that of ethanol and propanol but slower than that of water. As we will show in this study, the rate of proton transfer in methanol increases as the pressure increases up to about 1.9 GPa, the largest pressure used in this study. The pressure dependence of the proton transfer rate we find for methanol is similar to water, which is the best known solvent for protolytic reactions. The results, using methanol as a solvent, are consistent with our previous studies[32−35] of photoacids in water, ethanol, and propanol.

Experimental Section

Pressurized time-resolved emission was measured in a compact gasketed diamond anvil cell[36] (DAC) purchased from D'Anvil[37,38] with 0.3 carat low-fluorescent high-UV transmission diamonds.

To provide a larger volume of the sample for sufficient fluorescent intensity, a 0.45-mm hole was drilled in the 0.8-mm-thick stainless gasket. The low-fluorescence-type diamonds served as anvils. The anvil seats were with suitable circular apertures for the entry and exit of the exciting laser beam and the excited fluorescent intensity. With this cell, pressures up to 30 kbar were reached, without detriment to the diamond anvils. The pressure generated was calibrated using the well-known ruby fluorescent technique.[39]

Time-resolved fluorescence was acquired using the time-correlated single-photon counting (TCSPC) technique, the method of choice when sensitivity, a large dynamic range, and low-intensity illumination are important criteria in fluorescence decay measurements.

The TCSPC detection system is based on a Hamamatsu 3809U photomultiplier and Edinburgh Instruments TCC 900 computer module for TCSPC. The overall instrumental response was about 40 ps (full width at half-maximum, fwhm). Measurements were taken at 10-nm spectral width.

For excitation, we used two laser sources. The first laser is a cavity-dumped mode-locked Ti:sapphire femtosecond laser (Mira Coherent), which provides short (80 fs) pulses of variable repetition rate. We used the second harmonic generation (SHG) frequency over the spectral range 360−400 nm. The second laser system is a continuous wave (CW) mode-locked Nd:YAG pumped dye laser (Coherent Nd:YAG Antares and a 702 dye laser), operating with rohdamine 6G dye at a high repetition rate (1 MHz) of short pulses (2 ps at fwhm). The SHG of the rohdamine dye laser provides pulses (in the spectral range 285−313 nm) which were used to excite 2N68DS samples.

Steady-state fluorescence was measured using a FluoroMax-3 spectroflurimeter (Jobin Ivon).

2N68DS was purchased from Kodak. 10-CPT was purchased from ICN. DCN2 and 5CN2 were synthesized by Tolbert and co-workers.[40] The sample concentrations were between 4×10^{-4} and 1×10^{-4} M. Solvents were of reagent grade and used without further purification. All compounds were used without further purification. The pH of the solution was approximately 6.

The fluorescence spectrum of 2-naphthol-6,8-disulfonate consists of two structureless broad bands (∼40 nm fwhm). The emission band maximum of the acidic form (ROH*) of this naphtholsulfonate derivative in methanol emits at about 370 nm. The emission band maximum of the alkaline form (RO^-*) in methanol emits at about 460 nm. At 370 nm, the overlap of the two-luminescence bands is rather small, and the contribution of the RO^-* band to the total intensity at 370 nm is less than 1%. At 1 atm, the impurity and dimer emission level is about 0.2% of the peak intensity at 370 nm and increases to 1% at 10 kbar. Therefore, in the analysis of the time-resolved emission data, to the calculated signal we add an additional component with an exponential decay of about 10 ns and an amplitude of about 0.2% at 1 atm, which increases with pressure up to 1% at 10 kbar to account for the impurity fluorescence. To avoid ambiguity, because of the overlap between the fluorescence contributions of ROH* and RO^-* and in order to minimize the impurity fluorescence, we mainly monitored the ROH* fluorescence at 370 nm and the RO^-* fluorescence was monitored at 510 nm.

The DCN2 fluorescence spectrum consists of two structureless broad bands (∼40 nm fwhm). The emission band maximum of the acidic form (ROH*) in water and alcohols emits at 450 nm. The emission band maximum of the alkaline form (RO^-*) in water and alcohols emits at 600 nm. At 450 nm, the overlap of the two-luminescence bands is rather small, and the contribution of the RO^-* band to the total intensity at 450 nm is about 1%. In addition, we find some fluorescent impurity in the DCN2 compound that emits in the UV and blue parts of the emission spectrum. At 1 atm, the impurity emission level is about 1% of the peak intensity at 450 nm and increases to 3% at 20 kbar. The pressure dependence of the background luminescence can arise from dimerization of DCN2 to a nonproton emitting dimer. In the time-resolved analysis, to the calculated signal we add an additional component with an exponential decay of about 10 ns and an amplitude of about 1% at 1 atm, which increases with pressure up to 3% at 20 kbar to account for the impurity fluorescence.

Reversible and Irreversible Diffusion-Influenced Two-Step Model

Previous studies of reversible and irreversible ESPT processes in solution led to the development of a diffusion-influenced two-step model[41,42] (Scheme 1). In the continuous diffusion approach, the photoacid dissociation reaction is described by the spherically symmetric diffusion equation (DSE)[43] in three dimensions.[41,42] The boundary conditions at $r = a$ are those of the back reaction, (Scheme 1). k_{PT} and k_r are the "intrinsic" reversible (adiabatic) dissociation and recombination rate constants at the contact sphere radius, a. Quantitative agreement

SCHEME 1

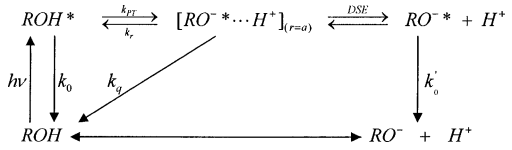

was obtained between the model and the experiment.[41,42] The back protonation may also proceed by a nonadiabatic, irreversible pathway involving proton quenching with a rate constant k_q.[3,44−47] From an analysis of the time-resolved data of the RO^- form of 5-cyano-2-naphthol, we find that quenching of the RO^- band affects the time-resolved emission profile of RO^-. A detailed description of the model, as well as the fitting procedure, is given in refs 13, 41, and 42.

Comparison of the numerical solution with the experimental results involves several parameters. Usually, the adjustable parameters are the proton transfer rate to the solvent, k_{PT}, and the geminate recombination rate, k_r. The contact radius, a, has acceptable literature values.[43] The proton dissociation rate constant, k_{PT}, is determined from the exponential decay at early times of the fluorescence decay. Over longer times, the fluorescence decay is nonexponential because of the reversible geminate recombination.

An important parameter in our model that strongly influences the nonexponential decay is the mutual diffusion coefficient, $D = D_{H^+} + D_{RO^-}$. The change in the proton conductivity in pressurized water is rather small. For methanol, ethanol, and propanol, the pressure dependence is unknown. In our previous studies, we estimated that D_{H^+} decreases with pressure by a factor of about 2 at 12 kbar. The proton diffusion constant, D_{H^+}, in methanol at atmospheric pressure, 295 K, is 0.27×10^{-4} cm^2/s. Another important parameter in the model is the Coulomb potential between the anion $RO^{-}{*}$ and the geminate proton.

$$V(r) = -\frac{R_D}{r} \qquad R_D = \frac{|z_1 z_2| e^2}{\epsilon_s k_B T} \tag{2}$$

where R_D is the Debye radius, z_1 and z_2 the charges of the proton and anion, ϵ_s the static dielectric constant of the solvent, T the absolute temperature, e the electronic charge, and k_B is Boltzmann's constant. We are not aware of any published data of the change in the dielectric constant of methanol with pressure. In ethanol, pentanol, and hexanol, it increases with pressure.[57] The relative increase of the dielectric constant with pressure, $\epsilon(P)/\epsilon_s$, where ϵ_s is the static dielectric constant at atmospheric pressure, roughly follows the change of the volume with pressure. For calculating $V(r)$, we assume that the relative dielectric constant, $\epsilon(P)/\epsilon_s$, in methanol changes as ethanol does with an increase in pressure.

The asymptotic expression (the long-time behavior) for the fluorescence of ROH*(t) is given by[41,48]

$$[\mathrm{ROH}^*] \cong \frac{\pi}{2} \alpha^2 \exp(R_D/a) \frac{k_r}{k_{PT}(\pi D)^{3/2}} t^{-3/2} \tag{3}$$

Equation 3 shows that uncertainty in the determination of $D(P)$ causes a larger uncertainty in k_r. Also, the fluorescence background, because of a fluorescent impurity and the band overlap, prevents us from accurately determining the recombination rate constant. We estimate that the error in the determination of k_{PT} is 10%. The error in the determination of k_{PT} is due to (1) the signal-to-noise ratio of the experimental signal, which affects the quality of the fluorescence signal over longer times and (2) the interplay between k_{PT} and k_r (see eq 3) over longer times. The uncertainty in the determination of k_r is estimated to be much larger, ~50%. The relatively large uncertainty in the values of k_r arises from the relation between k_r, $D(P)$, and $\epsilon(P)$. In this paper, we focus our attention on the pressure dependence of the proton dissociation rate constant, $k_{PT}(P)$, which is measured quite accurately.

Results

The Acid−Base Properties of 10-CPT and 2N68DS in Methanol Solution. Camptothecin (CPT) is a pentacyclic alkaloid, first isolated from extracts of the Chinese tree *Camptotheca acuminata*. This brightly fluorescent compound was found to be a potent inhibitor of the growth of leukemia cells by exhibiting a unique mechanism of action: inhibition of DNA topoisomerase I. A more potent water-soluble analogue of CPT, 10-hydroxycamptothecin (10-CPT), has a subunit

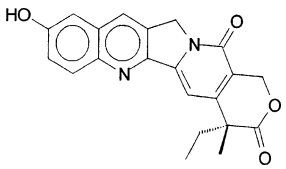

identical to 6-hydroxyquinoline (6HQ). Hydroxyquinoline derivatives are known to be both strong photoacids and strong photobases and, therefore, undergo efficient tautomerization in a very wide pH range, resulting in weak tautomer (zwitterion) emission.

The absorption and emission spectra of 10-CPT in water−methanol mixtures at room temperature (ca. 22 °C) in the pH range from neutral to basic, in general, exhibit a well-known naphthol-type behavior. The absorption spectra in neutral water and methanol are nearly identical, with the latter having a 3-nm bathochromic shift. The equilibrium between protonated (ROH, 380 nm) and deprotonated (RO^-, 420 nm) forms of 10-CPT is characterized by a pK_a of 8.9.

The emission spectra of 10-CPT in water−methanol mixtures exhibits dual fluorescence. The appearance of the low-energy emission band at 570 nm for 10-CPT water−methanol solution indicates an efficient PTTS process. The large fluorescence quantum yield and similarity of the emissions in neutral and basic solutions is evidence of the excited anion (RO^{*-}) formation, in contrast with 6HQ, for which double PTTS leads to the tautomer. In the water−methanol mixture with a 0.87 mole fraction of water, the inverse of the proton transfer rate is about 12 ps. In pure methanol, the dissociation rate is rather small, and its value is on the order of the excited-state lifetime of the ROH form in the absence of a proton transfer reaction.

Figure 1 shows the steady-state emission of 10-CPT in methanol, ethanol, and acetonitrile (a polar aprotic solvent). The relative RO^-/ROH emission band intensities are about 0.10 and 0.05 for methanol and ethanol solutions, respectively. In acetonitrile, the RO^- band is missing. Figure 2 shows the time-resolved emission of 10-CPT in acetonitrile, ethanol, and methanol, excited at 360 nm and measured at 440 nm, the ROH band maximum. The difference in the slope of the semilog plot of the fluorescence intensity versus time between acetonitrile and methanol reflects the existence of a proton transfer process in the protic solvents. The excited lifetime of the ROH form of 10-CPT in acetonitrile is 3.2 ns. The rate constant of proton transfer in methanol, at atmospheric pressure, was calculated to be 0.18 ns^{-1}.

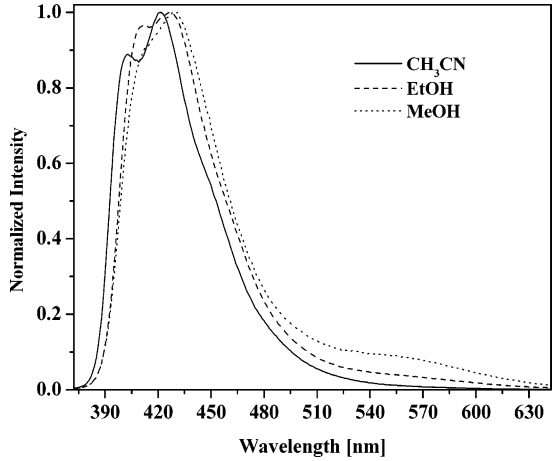

Figure 1. Steady-state emission of 10-CPT in neutral pH solution of acetonitrile (solid line), ethanol (dashed line), and methanol (dotted line). Note the emission band of the deprotonated form at 560 nm.

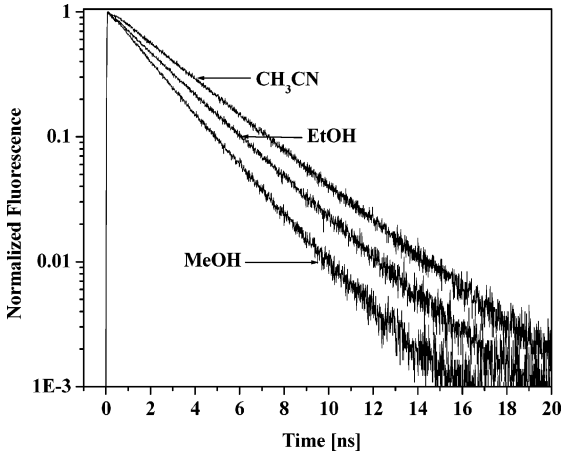

Figure 2. Time-resolved emission of 10-CPT excited at 360 nm and measured at 440 nm in three solvents.

2-Naphthol-6,8-disulfonate and 5-cyano-2-naphthol in water are relatively strong photoacids. The rate of proton transfer to water at atmospheric pressure and room temperature of both photoacids is about $(25\ \text{ps})^{-1}$. In methanol, the proton transfer rate of both photoacids is about 3 orders of magnitude smaller and thus comparable with the excited-state lifetime.

Time-Resolved Measurements of Photoacids in Pressurized Methanol. Figure 3a shows the time-resolved emission of the protonated form, ROH, of DCN2 in a methanol solution at various pressures in the range from 1 atm to 1.70 GPa measured at 470 nm. As the pressure increased, the short-time fluorescence decay rate increased. Figure 3b shows the time-resolved emission of the deprotonated form, RO^-, at various pressures measured at 630 nm. RO^- is the product of the excited-state protolytic dissociation of the photoacid ROH. The emission rise time depends on the pressure. The larger the pressure is, the faster the build-up time of the fluorescence. We used our model for proton transfer and reversible geminate recombination to fit the time-resolved emission experimental data for both the protonated and deprotonated forms. For quantitative fitting, we used the user-friendly SSDP program (version 2.63) of Krissnel and Agmon.[49] The computer fits to the experimental data are shown as solid lines in Figure 3a,b. The comparison of the calculated signal with the exponential results involves several parameters. The fitting parameters of the ROH and RO^{-}* emission curves of DCN2 in methanol are given in Table 1.

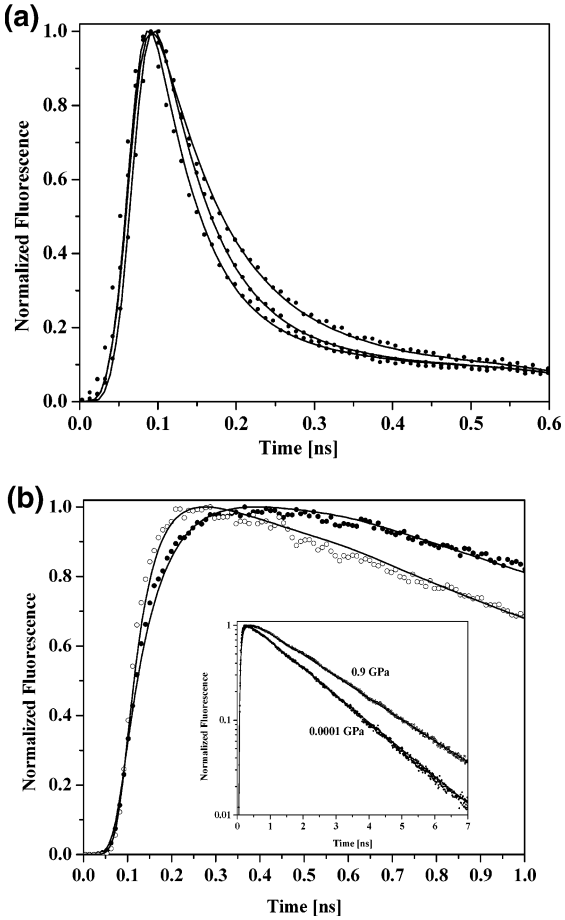

Figure 3. Time-resolved emission of DCN2 in methanol at various hydrostatic pressures. (a) The protonated ROH form at 1×10^{-4}, 0.40, and 1.18 GPa measured at 470 nm (from top to bottom). (b) The deprotonated RO^- form at 1×10^{-4} (●) and 0.9 (○) GPa measured at 630 nm.

TABLE 1: Pressure Dependence of the Kinetic Parameters for the Proton Transfer Reaction of DCN2 in Methanol

$P^{a,b}$ [GPa]	$k_{PT}{}^{c}$ [$10^9\ s^{-1}$]	$k_r{}^{c,d}$ [$10^9\ s^{-1}$]	D^e [$cm^2\ s^{-1}$]	R_D [Å]	$\tau_{ROH}{}^{-1}$ [ns^{-1}]	$\tau_{RO^-}{}^{-1}$ [ns^{-1}]
1×10^{-4}	12	7.5	2.8×10^{-5}	17	0.25	0.52
0.10	14	7	2.8×10^{-5}	17	0.25	0.52
0.20	16	8	2.7×10^{-5}	16.3	0.28	0.52
0.40	21	10	2.7×10^{-5}	15.5	0.30	0.56
0.90	22	13	2.5×10^{-5}	14.0	0.35	0.60
1.18	20	11.5	2.2×10^{-5}	13.5	0.42	0.66
1.35	19	12	2.2×10^{-5}	13.3	0.42	0.67

[a] 1 GPa ≈ 10 kbar. [b] The error in determination of the pressure is ±0.075 GPa. [c] k_{PT} and k_r are obtained from the fit of the experimental data by the reversible proton transfer model (see text). [d] The error in the determination of k_r is 50%; see text. [e] Values at high pressure obtained by best fit to the fluorescence decay.

We determined the proton transfer rate constant, k_{PT}, from the fit to the initial decay of the ROH* fluorescence. The initial decay is mainly determined by the deprotonation rate constant k_{PT} and is also sensitive to the geminate recombination rate constant k_r. The long-time behavior (the fluorescence tail) seen in the ROH* species is a consequence of the repopulation of ROH* by the reversible recombination of RO^{-}* with the geminate proton.

Figure 4a shows the time-resolved emission of the ROH form of 2N68DS in a methanol solution at various pressures in the range from 1 atm to 1.50 GPa. The samples were excited by 2-ps pulses at 310 nm and measured at 360 nm. Figure 4b shows

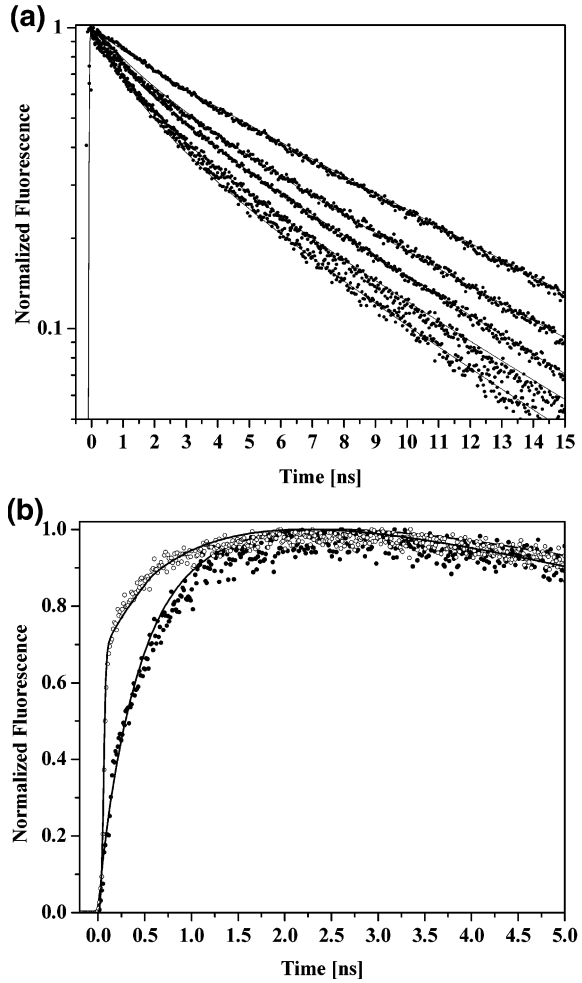

Figure 4. Time-resolved emission of 2-naphthol-6,8-disulfonate in methanol at various hydrostatic pressures. (a) The protonated ROH form at 1×10^{-4}, 0.55, 0.90, 1.30, and 1.50 GPa measured at 360 nm (from top to bottom). (b) The deprotonated RO^- form at 1×10^{-4} (●) and 1.30 (○) GPa measured at 500 nm.

the time-resolved emission of the RO^- form of 2N68DS at various pressures measured at 500 nm. We also show the fit (solid line) to the experimental results using the ESPT model. The value of the proton transfer rate constant k_{PT} is determined from the initial luminescence slope of ROH*. At low pressures, as the pressure increases, the slope increases and the proton transfer rate constant increases. The RO^-* rise time is also strongly affected by the pressure. As the pressure increases, the rise time is steeper. The fitting parameters of the time-resolved emission of both ROH and RO^- of 2N68DS at various pressures are given in Table 2.

Figure 5a shows the time-resolved emission and computer fit of the 10-CPT ROH form in methanol at various pressures. The sample was excited at 390 nm with ~100-fs pulses.

Figure 5b shows the time-resolved emission of the deprotonated form, RO^-, of 10-CPT in methanol measured at 600 nm. As seen from the figures, the initial decay of ROH increases with pressure, and the rise time of the RO^- is faster as the pressure increases. The fitting parameters of 10-CPT in methanol time-resolved emission are given in Table 3. Figure 6a,b shows the experimental results as well as the computer fits (solid line) of the time-resolved emissions of both the ROH and RO^- species of 5CN2 in methanol at various hydrostatic pressures. The fitting parameters are given in Table 4.

TABLE 2: Pressure Dependence of the Kinetic Parameters for the Proton Transfer Reaction of 2-Naphthol-6,8-disulfonate in Methanol

$P^{a,b}$ [GPa]	$k_{PT}{}^c$ [10^9 s^{-1}]	$k_r{}^{c,d}$ [10^9 s^{-1}]	D^e [cm^2 s^{-1}]	R_D [Å]	$\tau_{ROH}{}^{-1}$ [ns^{-1}]	$\tau_{RO^-}{}^{-1}$ [ns^{-1}]
1×10^{-4}	0.075	0.6	2.7×10^{-5}	50	0.115	0.150
0.11	0.08	0.35	2.7×10^{-5}	50	0.123	0.160
0.39	0.12	0.42	2.7×10^{-5}	46	0.105	0.105
0.55	0.18	0.5	2.7×10^{-5}	44	0.095	0.095
0.90	0.27	1	2.7×10^{-5}	41	0.1	0.118
1.30	0.37	1.05	2.7×10^{-5}	40	0.095	0.095
1.50	0.38	1	2.7×10^{-5}	38	0.105	0.1

[a] 1 GPa ≈ 10 kbar. [b] The error in determination of the pressure is ±0.075 GPa. [c] k_{PT} and k_r are obtained from the fit of the experimental data by the reversible proton transfer model (see text). [d] The error in the determination of k_r is 50%; see text. [e] Values at high pressure obtained by best fit to the fluorescence decay.

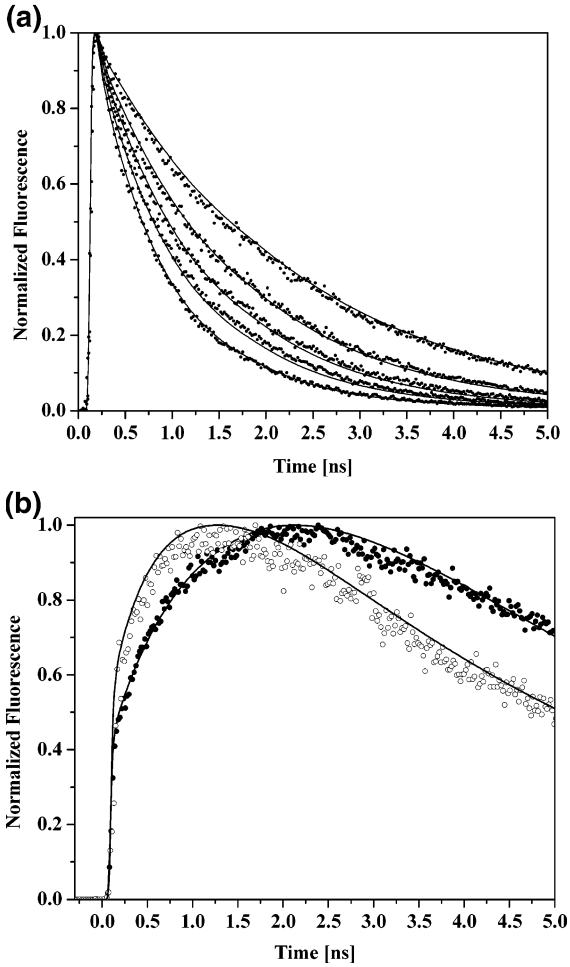

Figure 5. Time-resolved emission of 10-CPT in methanol at various pressures. (a) The protonated form of ROH at 1×10^{-4}, 0.25, 0.50, 0.75, and 1.00 GPa measured at 440 nm (from top to bottom). (b) The deprotonated form of RO^- at 1×10^{-4} (●) and 0.75 (○) GPa measured at 560 nm.

In all four compounds, the rate of proton transfer, k_{PT}, increases with pressure. At relatively low pressures, the change in the rate constant is large, while at high pressures, the rate of increase of k_{PT} with pressure is smaller.

Discussion

A Qualitative Model for the Temperature and Pressure Dependencies of Excited-State Proton Transfer Reactions. Previously, we used a qualitative model that accounts for both

TABLE 3: Pressure Dependence of the Kinetic Parameters for the Proton Transfer Reaction of 10-CPT in Methanol

$P^{a,b}$ [GPa]	$k_{PT}{}^{c}$ [10^9 s^{-1}]	$k_r{}^{c,d}$ [10^9 s^{-1}]	D^e [cm^2 s^{-1}]	R_D [Å]	$\tau_{ROH}{}^{-1}$ [ns^{-1}]	$\tau_{RO^-}{}^{-1}$ [ns^{-1}]
1×10^{-4}	0.18	0.18	3.2×10^{-5}	17	0.32	0.2
0.25	0.40	1.5	2.9×10^{-5}	16	0.32	0.2
0.50	0.60	2.0	2.8×10^{-5}	15	0.32	0.2
0.75	0.90	4.0	2.5×10^{-5}	14	0.32	0.2
1.00	1.10	4.1	2.3×10^{-5}	13.5	0.32	0.2

[a] 1 GPa ≈ 10 kbar. [b] The error in determination of the pressure is ±0.075 GPa. [c] k_{PT} and k_r are obtained from the fit of the experimental data by the reversible proton transfer model (see text). [d] The error in the determination of k_r is 50%; see text. [e] Values at high pressure obtained by best fit to the fluorescence decay.

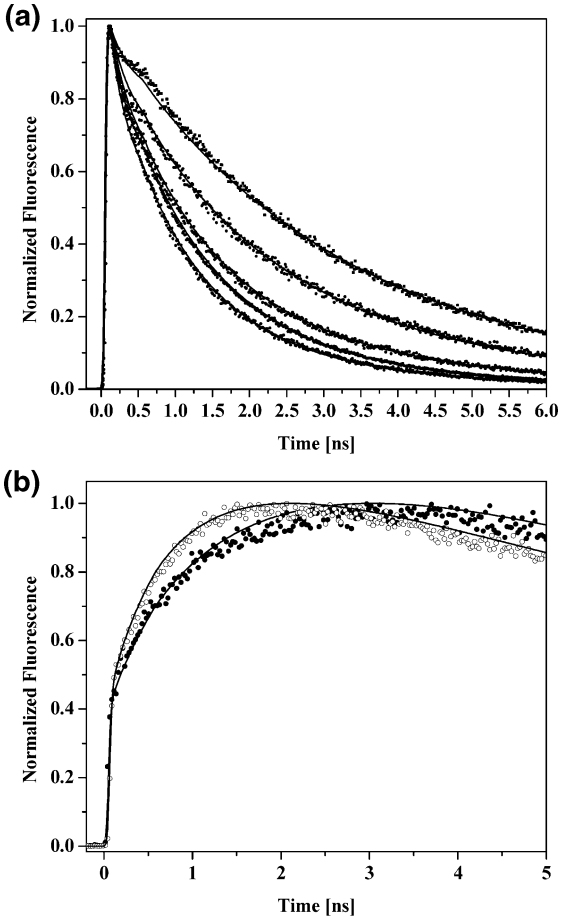

Figure 6. Time-resolved emission of 5-cyano-2-naphthol in methanol at various pressures. (a) The protonated form of ROH at 1×10^{-4}, 0.15, 0.39, 0.54, and 1.34 GPa measured at 420 nm (from top to bottom). (b) The deprotonated form of RO^- at 0.15 (●) and 0.54 (○) GPa measured at 530 nm.

the temperature[13−16] and, more recently,[32−35] the pressure dependences of the excited-state intermolecular proton transfer of photoacids to the solvents water, ethanol, and propanol. We shall use the same model to explain the pressure dependence of the proton transfer rate from 2N68DS, 10-CPT, 5CN2, and DCN2 to methanol. As described in the Introduction section, the proton transfer reaction depends on two coordinates, the first of which depends on the generalized solvent configuration. The solvent coordinate characteristic time, τ_S, is within the range of the dielectric relaxation time, τ_D, and τ_L, the longitudinal relaxation time. The second coordinate is the actual proton translational motion (tunneling) along the reaction path, q_H.

In the stepwise model, the overall proton transfer time is the sum of two times, $\tau = \tau_S + \tau_H$, where τ_S is the characteristic

TABLE 4: Pressure Dependence of the Kinetic Parameters for the Proton Transfer Reaction of 5CN2 in Methanol

$P^{a,b}$ [GPa]	$k_{PT}{}^{c}$ [10^9 s^{-1}]	$k_r{}^{c,d}$ [10^9 s^{-1}]	$k_q{}^{c,d}$ [10^9 Å s^{-1}]	D^e [cm^2 s^{-1}]	R_D [Å]	$\tau_{ROH}{}^{-1}$ [ns^{-1}]	$\tau_{RO^-}{}^{-1}$ [ns^{-1}]
1×10^{-4}	0.15	1.0	2.3	2.8×10^{-5}	17	0.19	0.12
0.15	0.45	7.0	3.0	2.8×10^{-5}	17	0.17	0.09
0.39	0.75	7.5	4.0	2.7×10^{-5}	16	0.17	0.075
0.54	0.86	8.2	5.0	2.7×10^{-5}	15.5	0.17	0.075
0.80	0.95	10.5	7.0	2.6×10^{-5}	14.0	0.17	0.075
1.03	1.30	18.0	8.5	2.4×10^{-5}	13.5	0.17	0.070
1.34	1.45	19.0	9.0	2.2×10^{-5}	13.3	0.17	0.070
1.53	1.45	19.0	9.0	2.1×10^{-5}	13.0	0.17	0.070

[a] 1 GPa ≈ 10 kbar. [b] The error in determination of the pressure is ±0.075 GPa. [c] k_{PT} and k_r are obtained from the fit of the experimental data by the reversible proton transfer model (see text). [d] The error in the determination of k_r is 50%; see text. [e] Values at high pressure obtained by best fit to the fluorescence decay.

time for the solvent reorganization and τ_H the time for the proton to pass to the acceptor. The overall rate constant, k_{PT}, at a given temperature, T, and pressure, P, is given by

$$k_{PT}(T, P) = \frac{k_H(T, P)k_S(T, P)}{k_H(T, P) + k_S(T, P)} \tag{4}$$

where $k_S(T, P)$ is the solvent coordinate rate constant and $k_H(T, P)$ the proton coordinate rate constant. Equation 4 provides the overall excited-state proton transfer rate constant along the lines of a stepwise process. Our stepwise model[14−18] for the overall proton transfer rate constant expression (eq 4) is similar to the expression of Rips and Jortner[50] for the overall electron transfer (ET) rate constant that bridges between the two extreme cases: nonadiabatic and adiabatic ET. The model restricts the proton transfer process to a stepwise one. The proton moves to the adjacent hydrogen-bonded solvent molecule only when the solvent configuration brings the system to the crossing point. As a solvent coordinate rate constant, we use

$$k_S(T, P) = b\frac{1}{\tau_D(T, P)} \tag{5}$$

where b is an adjustable empirical factor determined from the computer fit of the experimental data. We find that the empirical factor for monols lies between 2 and 4, while for water, it is larger and lies in the range 4−8. For the monols, τ_L is usually smaller than τ_D by a factor of 2−6 and for water by about a factor of 10. Thus, the solvent characteristic time, $\tau_S = 1/k_S(T, P)$, for water and monols lies between the dielectric relaxation and longitudinal times, $\tau_L < \tau_S < \tau_D$. The reaction rate constant, k_H, along the proton coordinate, q_H, is expressed by the usual activated chemical reaction description given by

$$k_H(P) = k_H^0(P)\exp\left(-\frac{\Delta G^{\ddagger}}{RT}\right) \tag{6}$$

where $k_H^0(P)$ is a pressure-dependent preexponential factor. For monols, at high enough temperature or, in the case of solvents with a large relaxation rate (which is the case for water, τ_D = 8 ps), the actual proton transfer along the proton tunneling coordinate, q_H, is the slower process and hence the rate-determining step. This rate strongly depends on pressure, because tunneling in the intermediate coupling case depends exponentially on the intermolecular distance between the two

heavy atoms. The activation energy, $\Delta G^{\ddagger}$, is determined by the Marcus relation

$$\Delta G^{\ddagger} = \frac{1}{4E_s}(E_s + \Delta G)^2 \qquad (7)$$

where E_s is the solvent reorganization energy and ΔG the free energy of the reaction. Thus, one needs to know the excited-state acid equilibrium constant, K_a^*, and the solvent reorganization energy. An alternative expression for $\Delta G^{\ddagger}$ can be evaluated from the structure reactivity relation of Agmon and Levine.[51] In our treatment, we assume that $\Delta G^{\ddagger}$ is independent of the hydrostatic pressure, and hence, the pressure solely affects the preexponential factor. In a previous study on the temperature dependence of the proton transfer rate from photoacids to water,[18] we found the activation energies for 2-naphthol ($pK^* = 2.7$) and 2N68DS ($pK^* = 0.4$) to be $\Delta G^{\ddagger} = 10$ and 2.5 kJ/mol, respectively. These values qualitatively agree with the Marcus expression for the activation energy (see eq 7), assuming reorganization energies in the range 0.1−0.3 eV. The proton transfer rates of 10-CPT, 2N68DS, and 5CN2 in methanol are about that of 2-naphthol in water. We therefore estimate that $\Delta G^{\ddagger}$ for these compounds in methanol is about that for 2-naphthol in water, $\Delta G^{\ddagger} = 10$ kJ/mol. For DCN2 in methanol, we estimate $\Delta G^{\ddagger} = 2.5$ kJ/mol.

$k_H(P)$ is related to the nonadiabatic limit rate expression. In the nonadiabatic limit, the preexponential factor is related to the tunneling coupling matrix element (see eq 1). The coupling matrix element depends strongly on the pressure and increases as the pressure increases.

Bromberg et al.[52] studied the effect of pressure and temperature on the photoinduced hydrogen transfer reaction in a mixed crystal of acridine in fluorene. The room temperature hydrogen transfer rate increases exponentially when pressure increases. On the basis of proton tunneling concepts, Trakhtenberg and Klochikhin[30] derived an expression for the pressure and temperature dependence of the tunneling rate of proton transfer in the solid state

$$k(T,P) = \nu \exp[-J(R_0) + J'R_0(1-\alpha_p^{-1/3}) + J'^2\delta_{CN}{}^2/8\alpha_p{}^{\gamma} \times \coth(\hbar\Omega_0\alpha_p{}^{\gamma}/4k_BT)] \qquad (8)$$

where $\alpha_P(P) = V_0/V(P)$, Ω_0 is the effective frequency of the intermolecular vibration, $\delta_{CN}{}^2$ is the square of the amplitude of the intercenter CN distance, and $\gamma = -\partial \ln \Omega_0/\partial \ln V$.

$$J(R) = (2/\hbar)\int_a^b \{2m[U(x,R) - E_H(R)]\}^{1/2}\,dx \qquad (9)$$

$E_H(R)$ and $U(x, R)$ are the total and potential energies of the tunneling atom respectively, depending on the distance, R, between the two heavy atoms (in our case, two oxygen atoms), and a and b are the coordinates of the barrier boundaries. R_0 is the equilibrium distance between the heavy atoms and J' the derivative, $\partial J/\partial R$. The first term on the right-hand side of eq 8 is the tunneling expression at atmospheric pressure and does not account for the pressure effect. The second term accounts for the change in the tunneling rate with pressure due to the change in the distance between the two heavy atoms. The third term takes into account the pressure effect on the intermolecular low-frequency modulation Ω_p. Trakhtenberg et al.[30] found good correspondence with the experimental results of Bromberg et al.[52] when they used a smaller power dependence of the compressibility, α_p (0.22 instead of $^1/_3$ as expected from the relation of distance and volume).

In recent studies, we measured, using time-resolved emission techniques, the proton dissociation from a strong photoacid, DCN2, as a function of pressure in both ethanol and propanol. In ethanol, we found that the proton dissociation rate constant, k_{PT}, of excited DCN2 at relatively low pressures (up to 7 kbar) increases with pressure. At about 7 kbar, it reaches the largest rate, about twice the rate at atmospheric pressure. At higher pressures, up to the freezing point of ethanol, about 1.9 GPa, the proton transfer rate decreases with pressure, and its value in the high-pressure regime is similar to the inverse of the dielectric relaxation time.

For propanol, we found that the proton dissociation rate constant, k_{PT}, of excited DCN2 at relatively low pressures (up to 5 kbar) increases slightly with pressure. At 5 kbar, the rate is 20% larger than the value at atmospheric pressure, while at higher pressures up to ∼2.5 GPa (25 kbar), the proton transfer rate decreases with pressure, and its value is related to the inverse of the dielectric relaxation time. At about 2.2 GPa, the rate is smaller, by a factor of about 20, than that at atmospheric pressure. The increase in the proton tunneling rate at low pressures increases the overall rate, k_{PT}, slightly. The solvent coordinate rate strongly affects k_{PT} at high pressures. At pressures above 5 kbar, k_{PT} is mainly determined by the solvent coordinate rate (i.e., the solvent-controlled limit).

In contrast with the strong pressure dependence on the solvent relaxation in propanol, pressure only mildly affects the solvent coordinate rate of water. In a recent study of the proton transfer from 2-naphthol and 2-naphtholmonosulfonate derivatives to water,[34,35] we found a strong increase of almost tenfold in the proton transfer rate, k_{PT}, with pressure.

The large difference in the pressure dependence of the proton transfer of DCN2 in propanol on one hand and naphtholmonosulfonate derivatives on the other hand arises from the delicate balance between $k_H(P)$ and $k_S(P)$. While $k_H(P)$ increases with pressure, $k_S(P)$ in propanol strongly decreases with pressure. In the case of DCN2 in propanol, the rate-limiting step is $k_S(P)$, and therefore, the proton transfer decreases with pressure. For naphtholsulfonate derivatives, in water $k_S(P)$ is big and almost insensitive to pressure. The rate-limiting step is $k_H(P)$, and the net result is a tenfold increase at 10kbar. $k_H(P)$ depends strongly on the change in the liquid volume with pressure, while $k_S(P)$ depends on the change of the viscosity with pressure.

Figure 7 shows the dependence of $1/\alpha_P = V_P/V_0$ on pressure for methanol. For comparison, we also added the pressure dependence of $1/\alpha_P$ for ethanol, propanol, and water, where V_P values for the liquids are taken from ref 57. The compressibility, $1/V(\partial V/\partial P)_T$, is a function of P. The volume decreases with an increase of pressure. As seen in Figure 7, the compressibility decreases strongly with pressure. In general, it is smaller for water than methanol and ethanol. For methanol and ethanol, it changes by factors of about 18 and 15, respectively, between atmospheric pressure and 12 kbar. The explanation of the large change in the compressibility of liquids in general is that, at low pressures, the molecules fit loosely together with considerable free space between them. The major part of the compressibility at low pressures arises from the occupancy of this free space. At high pressures, where the free space has become more or less squeezed out, this easy compressibility disappears, and the compressibility that remains is that furnished by the molecules themselves. As a first-order approximation, the change in intermolecular distance, δq_H, is related to the change in volume ΔV as $\sqrt[3]{\Delta V}$.

In our previous pressure studies of photoacids in water, ethanol, and propanol,[32−35,53] we estimated the pressure depen-

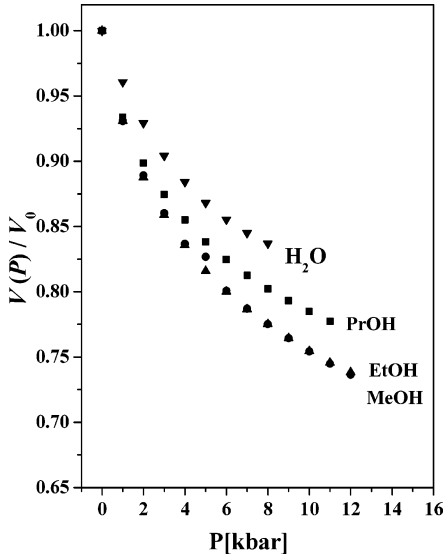

Figure 7. The pressure dependence of $1/\alpha_P = V_P/V_0$ of water, methanol, ethanol, and propanol at 293 K taken from ref 48.

dence of the proton coordinate rate constant, $k_H(P)$, from the second term of eq 8 with a compressibility dependence on power of 0.22 for ethanol and 0.27 for propanol.[32,33] For all photoacid−water systems discussed in refs 34 and 35, we used the value of 0.33,[35] because for the first approximation, $\delta q_H = \sqrt[3]{\Delta V}$. The contribution of the third term in eq 8 is rather small. For $\Omega_p = 5.0 \times 10^{13}$ s^{-1}, $\delta_{O-O}{}^2 = 0.005$ Å^2, $1/\alpha_P = V_P/V_0$, and $\gamma = 0.22$ (see ref 25), we find that the third term in eq 8 decreases the tunneling rate as the pressure increases. The rate decreases by about 30% at about 10 kbar. At higher pressures, the value of the third term is about the same as that at 10 kbar, because the volume compressibility is very small. In our treatment, we neglected the contribution to the pressure dependence of the third term in eq 8. Thus, the change in the proton tunneling rate constant as a function of pressure is given by

$$\frac{k_H(P)}{k_H(1\text{ atm})} \cong \exp[J'R_0(1 - \alpha_p{}^{-\xi}] \qquad (10)$$

where ξ is an adjustable parameter close to 0.33.

The rate increases as a function of pressure. Because the compressibility is not constant with pressure, but rather strongly decreases as the pressure increases, $k_H(P)/k_H(1\text{ atm})$ does not increase with the same initial slope.

Free energy relation[54−56] and temperature dependence experiments[15] indicated that the solvent fluctuation rate to equalize the energies in excited-state intermolecular proton transfer is not in the high-frequency range on the order of 10^{13} s^{-1}, (∼100−200 cm^{-1}), but rather slower than 10^{12} s^{-1}, (<10 cm^{-1}). For monols, diols, and glycerol, it is very close to $1/\tau_D$, where τ_D is the slow component of the dielectric relaxation time. We are not aware of literature-published values for the dielectric relaxation times as a function of pressure for methanol at higher pressures. In many cases, viscosity and τ_D have similar dependencies on both pressure and temperature. Figure 8 shows the viscosity dependence of methanol on pressure. For comparison, we also display the viscosity dependence on pressure in water, ethanol, and propanol.[57,58] Methanol, ethanol, and propanol exhibit a much stronger pressure dependence of the viscosity than water does. In water at 20 °C, the viscosity decreases slightly at low pressures, while at pressures above 2 kbar, the viscosity increases slightly. At 30 °C and higher

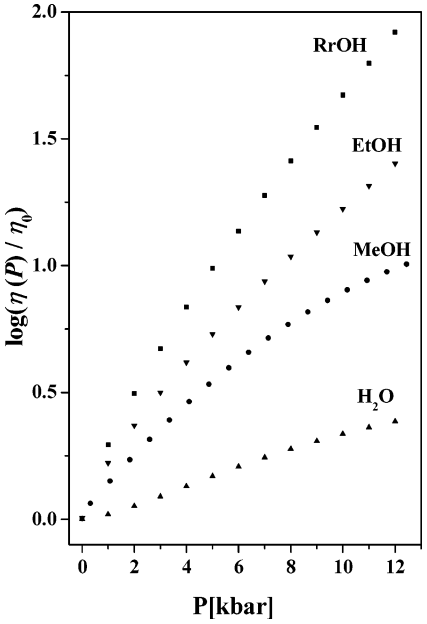

Figure 8. The viscosity dependence on the pressure of water, methanol, ethanol, and propanol at 303 K taken from ref 48. ▲, propanol data; ●, ethanol data; ■, methanol data; and ▼, water.

temperatures, the water viscosity slightly increases with pressure. In contrast with the pressure dependence of the viscosity of water, in propanol the viscosity depends strongly on pressure. It increases exponentially with the pressure increase in the pressure range 1 atm−12 kbar. At 12 kbar ($T = 303$ K), the viscosity is about 80 times larger than at 1 atm. The pressure dependence of the viscosity of methanol, the liquid we used in this study, is relatively small. At 30 °C, the viscosity at 12 kbar of methanol increased tenfold. The pressure dependence of the viscosity of ethanol is larger than methanol but smaller than propanol. The solvent relaxation rate is an important parameter in our qualitative two-coordinate stepwise model. We relate the solvent relaxation time, τ_s, to the dielectric relaxation time, τ_D.

The dielectric relaxation time is often directly proportional to the shear viscosity. This is a direct consequence of the assumed viscous-damped rotating sphere model of dielectric relaxation originally introduced by Debye.[43] In general, the viscosity dependence on pressure is larger than that of the dielectric relaxation. Johari and Danhauser studied the pressure dependence of the viscosity and the dielectric relaxation of isomeric octanols.[59,60] They found good correspondence between the pressure dependence of the viscosity and the dielectric relaxation times.

We used an approximate relation between $\tau_D(P)$ and $\eta(P)$ based on the correspondence between dielectric relaxation and $\eta(P)$ to estimate the pressure dependence of $\tau_D(P)$ of methanol.[34]

$$\tau_D(P) \approx \tau_D^{1\text{atm}} \times \left(\frac{\eta(P)}{\eta^{1\text{atm}}}\right) \times \exp(-P/P^*) \qquad (11)$$

For methanol at 1 atm and 20 °C, τ_D is about 60 ps. Because it is the best fit to the pressure dependence of k_{PT} using our stepwise model in methanol, we used a mild correction between $\tau_D(P)$ and $\eta(P)$ by introducing $P^* = 12\,000$ bar. Thus in methanol at about 12 kbar, the relaxation time $\tau_D(P)$ increases by about a factor of 4, while the viscosity increases by a factor of 10.

Figure 9 shows a fit to the stepwise two-coordinate model of $k_{PT}(P)$ as a function of pressure (solid line) along with the experimental data (dots) of 5CN2 and 2N68DS in methanol.

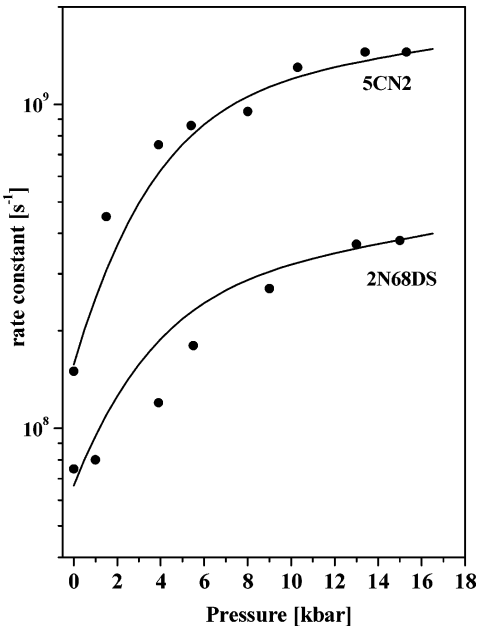

Figure 9. The pressure dependence of the proton transfer rate constant of 5CN2 and 2N68DS, along with the computed rate constant using eq 4.

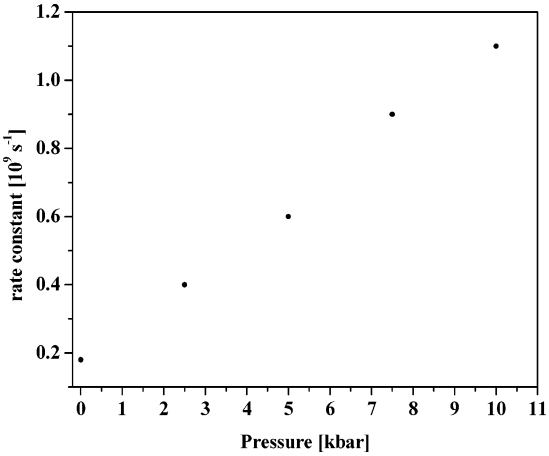

Figure 10. The experimental pressure dependence of the proton transfer rate constant of 10-CPT in methanol.

TABLE 5: Parameters for the Proton Transfer Rate Fittings

photoacid	$J'R_0$	$\Delta G^{\ddagger}$ [kJ/mol]	k_H(1 atm) [ns^{-1}]	ξ^a
DCN2	28	2.4	12	0.22
5CN2	32	10	0.15	0.25
2N68DS	27	10	0.075	0.22
10-CPT	30	10	0.18	0.20

[a] An adjustable parameter used in eq 10.

The results of 2N68DS and 5CN2 show an increase of the proton transfer rate with pressure increases. For 2N68DS in methanol, at about 17 kbar, the rate is 6 times larger than the rate at atmospheric pressure. Table 5 gives the fitting parameters of the model for the proton transfer rate of these compounds in methanol. The values of the parameters $J'R_0$ (see eq 10) range from 32 to 36. The value of the solvent relaxation parameter $b = 4$ for all calculations. Figure 10 shows the fit and experimental results of the proton transfer rate for 10-CPT in methanol. Figure 11 shows on a semilog plot the pressure dependence of DCN2 in methanol, ethanol, and propanol (the data for ethanol and propanol were taken from our previous studies[32,33]). The results

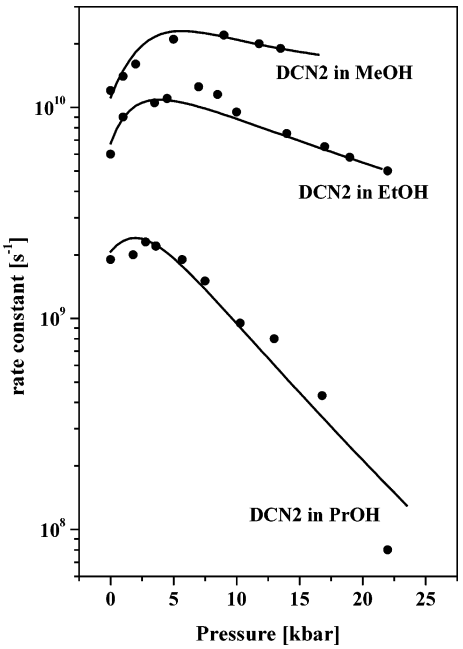

Figure 11. The pressure dependence of k_{PT} of DCN2 in methanol, ethanol, and propanol. The data of DCN2 in ethanol and propanol is taken from ref 34.

of DCN2 in methanol and ethanol show an initial increase of the rate with pressure. At about 8 kbar, the rate reaches a maximum value, $k_{PT}(8\ \text{kbar}) = 2k_{PT}(1\ \text{atm})$. A further pressure increase decreases slightly the rate of the proton transfer to the solvent. This pressure dependence observation of the proton transfer rate from DCN2 to methanol is quite similar to our previous finding in ethanol. It is explained by the opposite pressure dependencies of k_H and k_S and the saturation of k_H at medium pressure values of about 10 kbar. The results of DCN2 in propanol show only a slight increase of 20% of the proton transfer rate with pressure changes up to about 5 kbar. At pressures above 5 kbar (0.5 GPa), the rate decreases as a function of pressure. At about 2.2 GPa, the rate is smaller, by a factor of about 20, than that at atmospheric pressure.

Summary

We studied the pressure dependence of the excited-state proton transfer rate from photoacids to methanol, the protic solvent closest to water in both its protic properties and its solvent relaxation rate, which is faster than that of ethanol and propanol.

Time-resolved emission techniques were employed to measure the proton dissociation and reversible geminate recombination from photoacids 2-naphthol-6,8-disulfonate, 10-camptothecin, 5-cyano-2-naphthol, and 5,8-dicyano-2-naphthol to methanol as a function of pressure. We used a stepwise two-coordinate model to qualitatively fit the pressure dependence of the proton transfer rate. We previously used this model to successfully explain both the temperature and pressure dependences of the proton transfer rate from various photoacids to solvents.[13−17,32−35] The explanation for the large difference between the pressure dependence of the proton transfer rate from the relatively weak photoacids 10-CPT, 2N68DS, and 5CN2 to methanol and that from the stronger photoacid DCN2 to methanol, ethanol, and propanol is given along the lines of the stepwise two-coordinate proton transfer model.

The analysis of the experimental data by the model shows that the pressure affects both steps but in opposite directions.

Pressure decreases the solvent coordinate rate, k_S. In contrast to k_S, the tunneling rate, k_H, in methanol increases almost tenfold with pressure. In methanol, k_S is large and k_H for the photoacids we studied is small, and hence, the rate-determining step is k_H.

1. We found that the proton dissociation rate constant, k_{PT}, of excited DCN2 in methanol increases with pressure increase by a factor of 2 of about 0.9 GPa. At pressure above 1 GPa, the rate slightly decreases with further increase of external pressure.

2. The rate constant k_{PT} for 5CN2 in methanol increases by about a factor of 8 when pressure increases to about 1 GPa. The proton transfer rate is almost insensitive to further pressure increase.

3. In the case of 2N68DS in methanol, the proton transfer rate increases with pressure. At about 1.50 GPa (15 kbar), the rate constant is larger by a factor of about 6 than the value at atmospheric pressure.

4. In the case of 10-CPT, the rate increases by a factor of about 5 at a pressure of about 1.3 GPa.

These results, using methanol as a solvent, are consistent with our previous studies[32−35] of photoacids in water, ethanol, and propanol.

Acknowledgment. We thank Prof. L. M. Tolbert for providing the DCN2 and 5CN2 compounds. We thank Prof. M. Pasternak and Dr. G. Rozenberg for providing the diamond anvil cell high-pressure technology. This work was supported by grants from the U.S.−Israel Binational Science Foundation and the James-Franck German−Israel Program in Laser−Matter Interaction.

References and Notes

(1) Weller, A. *Prog. React. Kinet.* **1961**, *1*, 189.
(2) Förster, Th.; Volker, S. *Chem. Phys. Lett.* **1975**, *34*, 1.
(3) Ireland, J. F.; Wyatt, P. A. H. *Adv. Phys. Org. Chem.* **1976**, *12*, 131.
(4) Shizuka, H. *Acc. Chem. Res*. **1985**, *18*, 141.
(5) Arnaut, L. G.; Formosinho, S. J. *J. Photochem. Photobiol., A* **1993**, *75*, 1.
(6) Tolbert, L. M.; Solntsev, K. M. *Acc. Chem. Res*. **2002**, *35*, 19.
(7) Huppert, D.; Gutman, M.; Kaufmann, K. J. In *Advances in Chemical Physics*; Jortner, J., Levine, R. D., Rice, S. A., Eds.; Wiley: New York, 1981; Vol. 47, p 681. Kosower, E. M.; Huppert, D. In *Annual Reviews of Physical Chemistry*; Strauss, H. L., Babcok, G. T., Moore C. B., Eds.; Annual Reviews, Inc.: Palo Alto, CA, 1986; Vol. 37, p 122.
(8) Lee, J.; Robinson, G. W.; Webb, S. P.; Philips, L. A.; Clark, J. H. *J. Am. Chem. Soc.* **1986**, *108*, 6538.
(9) Gutman, M.; Nachliel, E. *Biochim. Biophys. Acta* **1990**, *391*, 1015.
(10) Agmon, N. *J. Phys. Chem.* **2005**, *109*, 13.
(11) Knochenmuss, R. *Chem. Phys. Lett.* **1998**, *293*, 191.
(12) Peters, S.; Cashin, A.; Timbers, P. *J. Am. Chem. Soc*. **2000**, *122*, 107.
(13) Poles, E.; Cohen, B.; Huppert, D. *Isr. J. Chem*. **1999**, *39*, 347.
(14) Cohen, B.; Huppert, D. *J. Phys. Chem. A* **2000**, *104*, 2663.
(15) Cohen, B.; Huppert, D. *J. Phys. Chem. A* **2001**, *105*, 2980.
(16) Cohen, B.; Huppert, D. *J. Phys. Chem.* **2002**, *106*, 1946−1955.
(17) Cohen, B.; Segal, J.; Huppert D. *J. Phys. Chem. A* **2002**, *106*, 7462−7467.
(18) Cohen, B.; Leiderman, P.; Huppert, D. *J. Phys. Chem. A* **2002**, *106*, 11115−11122.
(19) Kolodney, E.; Huppert, D. *J. Chem. Phys.* **1981**, *63*, 401.
(20) Ando, K.; Hynes, J. T. In *Structure, energetics and reactivity in aqueous solution*; Cramer, C. J., Truhlar, D. G., Eds.; ACS Symposium Series; American Chemical Society: Washington, DC, 1994.
(21) Agmon, N.; Huppert, D.; Masad, A.; Pines, E. *J. Phys. Chem.* **1991**, *96*, 952.
(22) German, E. D.; Kuznetsov, A. M.; Dogonadze, R. R. *J. Chem. Soc*., *Faraday Trans. 2* **1980**, *76*, 1128.
(23) Kuznetsov, A. M. *Charge Transfer in Physics, Chemistry and Biology*; Gordon and Breach: Langhorn, PA, 1995.
(24) Borgis, D.; Hynes, J. T. *J. Phys. Chem.* **1996**, *100*, 1118. Borgis, D. C.; Lee, S.; Hynes, J. T. *Chem. Phys. Lett.* **1989**, *162*, 19. Borgis, D.; Hynes, J. T. *J. Chem. Phys.* **1991**, *94*, 3619.
(25) Kiefer, P. M.; Hynes, J. T. Accepted for publication in *Solid State Ionics*.
(26) Cukier, R. I.; Morillo, M. *J. Chem. Phys.* **1989**, 91, 857. Morillo, M.; Cukier, R. I. *J. Chem. Phys.* **1990**, *92*, 4833.
(27) Li, D.; Voth, G. A. *J. Phys. Chem.* **1991**, *9*, 5, 10425. Lobaugh, J.; Voth, G. A. *J. Chem. Phys.* **1994**, *100*, 3039.
(28) Hammes-Schiffer, S. *Acc. Chem. Res*. **2001**, *34*, 273.
(29) Ando, K.; Hynes, J. T. *J. Phys. Chem. B* **1997**, *101*, 10464.
(30) Trakhtenberg, L. I.; Klochikhin, V. L. *Chem. Phys.* **1998**, *232*, 175.
(31) Goldanskii, V. I.; Trakhtenberg, L. I.; Fleuorov, V. N. *Tunneling Phenomena in Chemical Physics*; Gordon and Breach: New York, 1989; Chapter 4.
(32) Koifman, N.; Cohen, B.; Huppert, D. *J. Phys. Chem A* **2002**, *106*, 4336.
(33) Genosar, L.; Leiderman, P.; Koifman, N.; Huppert, D. *J. Phys. Chem A* **2004**, *108*, 309.
(34) Genosar, L.; Leiderman, P.; Koifman, N.; Huppert, D. *J. Phys. Chem A* **2004**, *108*, 1779.
(35) Leiderman, P.; Genosar, L.; Koifman, N.; Huppert, D. *J. Phys. Chem A* **2004**, *108*, 2559.
(36) Jayaraman, A. *Rev. Mod. Phys.* **1983**, *55*, 65.
(37) Machavariani, G. Yu.; Pasternak, M. P.; Hearne, G. R.; Rozenberg, G. Kh. *Rev. Sci. Instrum.* **1998**, *69*, 1423.
(38) D'Anvils is administered by Ramot, Ltd., 32 H. Levanon Str., Tel Aviv 61392, Israel. http://www.tau.ac.il/ramot/danvils.
(39) Barnett, J. D.; Block, S.; Piermarini, G. J. *Rev. Sci. Instum.* **1973**, *44*, 1.
(40) Tolbert, L. M.; Haubrich, J. E. *J. Am. Chem. Soc.* **1990**, *112*, 8163; **1994**, *116*, 10593.
(41) Agmon, N.; Pines, E.; Huppert, D. *J. Chem. Phys.* **1988**, *88*, 5631.
(42) Pines, E.; Huppert, D.; Agmon, N. *J. Chem. Phys.* **1988**, *88*, 5620.
(43) Debye, P. *Trans. Electrochem. Soc.* **1942**, *82*, 265
(44) Masad, A.; Huppert, D. *Chem. Phys. Lett.* **1991**, *180*, 409.
(45) Pines, E.; Tepper, D.; Magnes, B.-Z.; Pines, D.; Barak, T. *Ber Bunsen-Ges.* **1998**, *102*, 504.
(46) Solntsev, K. M.; Huppert, D.; Agmon, N. *J. Phys. Chem.* **1999**, *103*, 6984.
(47) Solntsev, K. M.; Huppert, D.; Agmon, N.; Tolbert, L. M. *J. Phys. Chem. A* **2000**, *104*, 4658.
(48) Agmon, N.; Goldberg, S. Y.; Huppert, D. *J. Mol. Liq.* **1995**, *64*, 161.
(49) Krissinel, E. B.; Agmon, N. *J. Comput. Chem*. **1996**, *17*, 1085.
(50) Rips, I.; Jortner, J. *J. Chem. Phys.* **1987**, *87*, 2090.
(51) Agmon, N.; Levine, R. D. *Chem. Phys. Lett.* **1977**, *52*, 197; *Isr. J. Chem.* **1980**, *19*, 330.
(52) Bromberg, S.; Chan, I.; Schilke, D.; Stehlik, D. *J. Chem. Phys.* **1993**, *98*, 6284.
(53) Cohen, B.; Leiderman, P.; Huppert. D. *J. Lumin.* **2003**, *102−103*, 676.
(54) Pines, E.; Fleming, G. R. *Chem. Phys. Lett.* **1994**, *183*, 393.
(55) Pines, E.; Magnes, B.; Lang, M. J.; Fleming, G. R. *Chem. Phys. Lett.* **1997**, *281*, 413.
(56) Solntsev, K.; Huppert, D.; Agmon, N. *J. Phys. Chem. A* **2000**, *104*, 4658.
(57) Bridgman, P. E. *The Physics of High Pressure*; G. Bell and Sons, Ltd.: London, 1958.
(58) Andrussow, L.; Schramm, B. In Landolt-Börnstein; Schaffer, K., Ed.; Springer: Berlin, 1969; Part 5a, Vol. 2.
(59) Johari, G.; Dannhauser, W. *J. Chem. Phys.* **1969**, *50*, 1862.
(60) Johari, G.; Dannhauser, W. *J. Chem. Phys.* **1969**, *51*, 1626.